Hybrid atomistic-continuum fluid mechanics

T. Werder, J. H. Walther, E. Kotsalis, P. Gonnet and P. Koumoutsakos

Institute of Computational Science, ETH Zürich
Hirschengraben 84, 8092 Zürich, Switzerland
{werder,walther,kotsalis,gonnetp,koumoutsakos}@inf.ethz.ch

ABSTRACT

We outline a multiscale algorithm for the simulation of dense fluids that couples molecular dynamics and continuum fluid dynamics. The coupling between the two models is realized by a common overlap domain and by the alternating Schwarz method. We prefer this method to those based on direct flux exchange, since the accurate estimation of the fluxes requires much more statistics. The boundary conditions on the atomistic region are imposed using stochastic walls to thermalize and confine the molecular dynamics system, and the USHER algorithm to insert new atoms. The forcing of the continuum is achieved using appropriate source terms in the momentum equations. To test the algorithm, we study equilibrium liquid argon systems and the flow of liquid argon past a carbon nanotube.

Keywords: multiscale algorithm, molecular dynamics, fluid dynamics

1 Introduction

The study of fluid mechanics at the nanoscale level [1] has received wide attention due to its importance for the understanding and development of biosensors. From the computational side, classical molecular dynamics (MD) have so far been the most useful tool to characterize phenomena such as wetting, hydrophobicity and boundary conditions. One system of particular interest with regard to biosensors is carbon nanotubes in water, which has recently been studied in some detail [2], [3]. Despite the success of molecular dynamics, its limitations in terms of accessible length and time scales are currently of the order of $10\,\mathrm{nm}^3$ and $10\,\mathrm{ns}$. In order to allow the computational analysis of nanoscale systems integrated in microfluidic environments, a multiscale approach is indispensable for the following two reasons. First, even with special purpose parallel hardware and state of the art algorithms, it remains prohibitively expensive to reach the microscale using classical MD simulations. Second, the amount of data that such a computation would generate is intractable.

For both dilute [4], and dense fluids [5]–[7] different algorithms exist to couple atomistic and continuum simulations. Here, we present an algorithm to impose arbitrary, non-periodic boundary conditions on MD simulations of dense fluids, cf. Fig. 1. We show how this algorithm couples standard molecular dynamics codes with commercial computational fluid dynamics packages. As a first application we consider a flow of liquid argon around a carbon nanotube (CNT), where only the CNT and its interaction with the nearby argon are modeled using MD, cf. Fig. 4, and where the continuum part is described by the isothermal, incompressible, Navier-Stokes (NS) equations.

2 The computational method

The central part of any hybrid scheme is the coupling of the atomistic and continuum regions. One can distinguish between two fundamental types of coupling, the former aim at matching the fluxes of mass, momentum, and energy at the interface [6], [7] and, the others are based on overlapping cells where the mass density ρ, the mean velocity $\boldsymbol{u}$, and the temperature T are imposed. The latter schemes have two main advantages over flux based schemes, namely that they decouple time scales [5] and that densities are substantially easier to sample than fluxes. This can be quantified by the number of atomistic samples M_q required to achieve a statistical error E_q in a quantity q measured in a domain of volume V [8], where E_q is defined as $E_q = \sigma(\bar{q})/\bar{q} = \sigma(q)/\sqrt{M}\bar{q}$, and where $\bar{q}$ and $\sigma(q)$ denote the average and standard deviation of q. Recently, estimates were given for the number of samples needed for the mean velocity, the density, and the pressure [8]

$$M_u = \frac{k_B T_0}{\bar{u}_x^2} \frac{1}{\rho V {E_u}^2}, \tag{1}$$

$$M_\rho = \frac{\kappa_T k_B T_0}{V {E_\rho}^2}, \tag{2}$$

$$M_P = \frac{\gamma k_B T_0}{P_0^2 \kappa_T} \frac{1}{V {E_P}^2}. \tag{3}$$

To illustrate Eqns. (1)-(3), consider the following numerical example: Assume we measure $\boldsymbol{u}$, ρ, and the pressure P of bulk water in a cell of volume $1\,\mathrm{nm}^3$ at atmospheric conditions ($P = 1\mathrm{bar}$, $T = 293\,\mathrm{K}$) and with a ratio of specific heats $\gamma = 1$, an isothermal compressibility of $\kappa_T = 48.95 \cdot 10^{-6}\,\mathrm{bar}^{-1}$, and a mean velocity

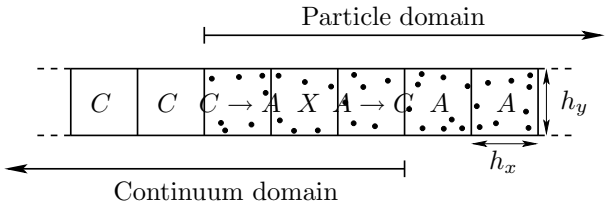

Figure 1: One dimensional sketch of a computational domain. There are pure continuum (C) and particle cells (A), as well as overlap cells $C \to A$, X, and $A \to C$, where both descriptions are valid. The Schwarz iteration by turns imposes the values measured in the $C \to A$ cells on the atomistic region and the values measured in the $A \to C$ cells on the continuum region until the solution converges in X.

$\bar{u}_x = 100\,\mathrm{ms}^{-1}$. Then, to obtain a fractional error of 5% the number of required (*statistically independent*) samples amounts to $M_u \approx 10^2$, $M_\rho \approx 1$, and $M_P \approx 10^8$. We note that the pressure is particularly expensive to sample and that we therefore favour density based schemes, where the pressure does not need to be computed or imposed directly.

2.1 The Schwarz algorithm

The algorithm is based on the Schwarz iteration scheme [5], i.e., the computational domain consists of continuum cells C, particle cells A, and overlap cells X, where both descriptions are valid, cf. Figs. 1 and 2. The following iteration is run until the solution is converged in the overlap region.

Step 1) Run an MD simulation until a steady state is reached, with $(\rho, \boldsymbol{u}, T)$ imposed in the $C \to A$ cells.

Step 2) Solve the continuum equations with the steady state solution of the MD in the $A \to C$ cells as boundary conditions.

2.2 The atomistic part

The main difficulties in imposing the continuum field values on the atomistic system in the $C \to A$ domain are the introduction and removal of particles but also the altered dynamics of the molecules in the $C \to A$ region due to the "missing particles" exteriour to the atomistic domain. For a monatomic Lennard-Jones fluid, the first problem is solved using the USHER algorithm [9]. For the second problem, we use the notion of stochastic boundary condition introduced to simulate the contact of an MD system with a thermal reservoir [10]. A generic molecular dynamics time step, where $(\rho, \boldsymbol{u}, T)$ are given in the $C \to A$ cells, reads:

1. *Force computation.* Compute forces according to the pair potential U and the wall force $F_{\mathrm{w}}(x)$.

2. *Velocity update.* Update the particle velocities using the leap-frog scheme.

3. *Andersen thermostat.* Choose particles randomly in the $C \to A$ cells with probability ν. Reset their instantaneous velocities $\widetilde{u}$ according to a biased Maxwell-Boltzmann distribution with a mean velocity $\boldsymbol{u}$ and temperature T.

$$f(\widetilde{u}_k) = \sqrt{\frac{m}{2\pi k_b T}} \exp\left(-\frac{(\widetilde{u}_k - u)^2}{2k_b T}\right). \quad (4)$$

4. *Position update.* Update the particle positions using the leap-frog scheme.

5. *Stochastic wall.* The boundary between $C \to A$ and C cells is formed by a stochastic wall W [10]. The normal velocity of particles k that hit W is sampled from the probability density [12]

$$f(\widetilde{u}_k) = \frac{m}{k_b T}|u_k| \exp\left(-\frac{(\widetilde{u}_k - u)^2}{2k_b T}\right), \quad (5)$$

and the tangential components are sampled from Eq. (4).

6. *Mass flux.* We consider an incompressible system and ensure mass conservation by collecting and redistributing the particles that leave the atomistic domain. Note that the particles are not periodically mapped, but they are re-introduced in the cell with the lowest instantaneous density using the USHER algorithm [9]

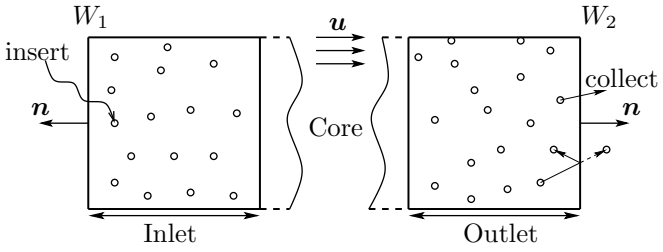

Figure 2: Schematic representation of an atomistic simulation domain with non-periodic boundary conditions. In the core region an NVE molecular dynamics simulation is performed, while the inlet and outlet are thermostatted at a temperature T and with mean velocity $\boldsymbol{u}$. W_1 and W_2 denote the positions of the stochastic walls. The outward normal $\boldsymbol{n}$ points toward the continuum region.

2.3 The continuum part

The continuum system is described by a finite volume discretization of the isothermal, incompressible, Navier-Stokes (NS) equations in the entire computational domain including the atomistic region. By the complete

overlay, we avoid explicit internal interfaces in the continuum system and instead utilize body forces to impose the average molecular velocity field. We note that the external boundary conditions of the continuum system are not limited to cyclic conditions, but can take any for the flow solver admissible form.

The x-component of the discrete momentum equation reads

$$A_P^x u_P^x + \sum_i^N A_i^x u_i^x + S_1^x = 0, \qquad (6)$$

where the sum includes the contributions from the N neighboring finite volumes. The coefficients (A_i) in Eq. (6) contain convective and diffusive fluxes across the cell faces which determine the total change of the cell velocity field. The central coefficient is given by $A_P = \sum_i A_i + S_2$, where S_1 and S_2 denote the contribution from body forces per unit volume within the cell, e.g., $B^x = S_1^x + S_2^x u_P^x$. For incompressible flow, an equation for the pressure is derived using the SIMPLE method [13]. The velocity field is imposed by choosing $S_1 = 10^{30}$ and $S_2 = -10^{30}$.

Here, with the assumptions of an isothermal, incompressible fluid, we solely need to extract the mean velocity from the atomistic domain. Since in general, the macroscopic time scale τ_C on which $\boldsymbol{u}$ changes is much larger than the microscopic time scale τ_P, $\boldsymbol{u}$ is simply taken to be the time averaged mean velocity. If $\tau_P/\tau_C \approx 1$, then a statistically relevant ensemble average can be reached through multiple realizations of a short simulation with perturbed initial conditions.

3 Results

To test the proposed algorithm, we have interfaced a Navier-Stokes solver (StarCD [14]), with an in-house molecular dynamics code (FASTTUBE [15]). We consider liquid argon systems in equilibrium and flowing past a carbon nanotube. The argon interacts through a Lennard-Jones pair potential

$$V(r) = 4\epsilon_{\alpha\beta}\left[\left(\frac{\sigma_{\alpha\beta}}{r}\right)^{12} - \left(\frac{\sigma_{\alpha\beta}}{r}\right)^{6}\right], \qquad (7)$$

where $\epsilon_{\alpha\beta}$ and $\sigma_{\alpha\beta}$ denote the Lennard-Jones parameters for the species α and β. For the argon-argon interaction, we use coefficients of $\epsilon_{\mathrm{ArAr}} = 1.0\,\mathrm{kJ\,mol^{-1}}$ and $\sigma_{\mathrm{ArAr}} = 0.34\,\mathrm{nm}$. The carbon nanotube is modeled as a rigid structure which interacts with the argon through a Lennard-Jones potential with coefficients $\epsilon_{\mathrm{CAr}} = 0.57\,\mathrm{kJ\,mol^{-1}}$ and $\sigma_{\mathrm{CAr}} = 0.34\,\mathrm{nm}$.

3.1 Equilibrium systems

To validate the proposed algorithm, we consider an equilibrium system of 1589 argon atoms at 300 K in a computational box of dimensions $5 \times 5 \times 5\,\mathrm{nm}$. The y and z-directions are treated periodically, while for the x-direction, the following variants were considered: (i) periodic boundary conditions (PBC) as a reference solution, (ii) PBC but with a stochastic wall (SW), and (iii) a non-periodic system with SW. Figure 3 displays for these different cases the mass density along the x-axis (only leftmost part shown) measured in bins of thickness 0.05 nm and averaged over 500 snapshots (taken every 0.2 ps). We note that the stochastic wall alone does not disturb the averaged local density field. However, for the non-periodic system (iii), we observe a layering of the liquid near the wall. Toward the bulk system, the layering decays quickly and is not expected to affect the bulk properties.

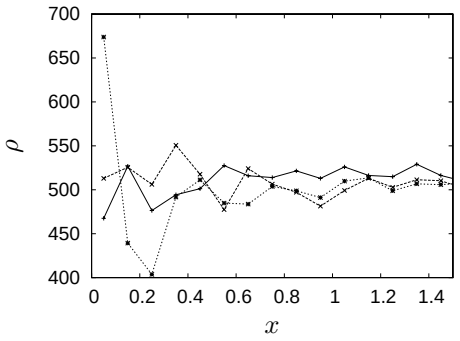

Figure 3: Density profiles extracted from equilibrium atomistic simulations with different boundary conditions (BC) at $x \leq 0$: Periodic BC ($\diamond$), periodic BC with a stochastic wall ($+$), and non-periodic with a stochastic wall ($\square$).

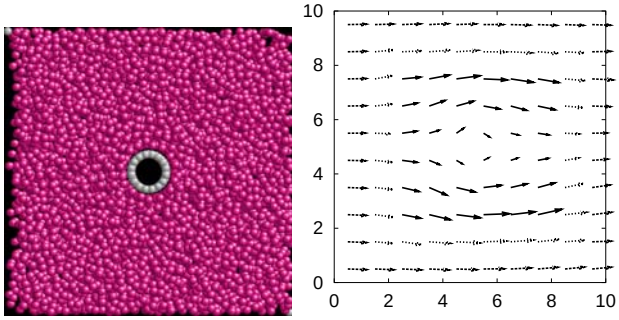

Figure 4: Flow of argon around a carbon nanotube. Left: A snapshot of the atomistic system. Right: The converged velocity field in the atomistic domain. The continuum domain is not shown.

3.2 Flow of liquid argon around a carbon nanotube

For the study of a flow around a carbon nanotube, we choose the size of the finite-volume cells to match the size and location of the bins used in the molecular

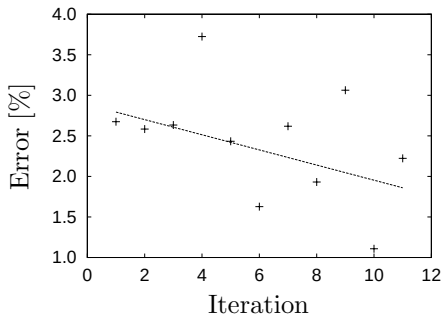

Figure 5: Convergence of the velocity field imposed on the edge of the atomistic domain. The error measure is defined in Eqn. (8). The solid line is a linear fit to the data.

system for the averaging and for the imposition of the boundary conditions. In the present study we use cells of size $1.0 \times 1.0 \times 4.26\,\mathrm{nm}$ to secure a sufficient averaging and forcing of the molecular system. The continuum mesh consists of $30 \times 30 \times 1$ mesh points. The boundary conditions of the continuum system are chosen to be periodic in y and z. A flow is imposed along the x-direction with an inlet velocity of $u_x = 100\,\mathrm{ms}^{-1}$ at the left boundary and an outlet boundary condition at the right boundary. The atomistic domain extends over $10 \times 10 \times 4.26\,\mathrm{nm}$ (including the $C \rightarrow A$ cells) and contains 5600 argon atoms. Finally, the carbon nanotube is of chirality (16,0) and oriented along the z-axis. A snapshot of the atomistic domain is given in Fig. 4.

In every iteration of the atomistic domain, we let the system adapt to the new boundary conditions for 20 ps, and we subsequently sample the system during 80 ps.

We quantify the convergence through the measure

$$e^k = \frac{1}{N} \sum_{i=1}^{N} \frac{|\boldsymbol{u}_i^k - \boldsymbol{u}_i^{k-1}|}{|\boldsymbol{u}_i^{k-1}|} \qquad (8)$$

where $\boldsymbol{u}_i^k$ is the mean velocity imposed on the i'th of N $C \rightarrow A$ cells in the k'th iteration. In Fig. 5, we show this measure as a function of the iteration number. The fractional error in sampling the velocity in the atomistic region is estimated to be $\approx 2.5\%$. Therefore we conclude that the solution has nearly converged after the first iteration, cf. Fig. 5.

4 Conclusion and Outlook

We have presented a hybrid multiscale algorithm for the coupling of atomistic and continuum systems. It is based on the Schwarz domain decomposition technique, the Usher algorithm for particle insertions, and stochastic walls. Future work includes the extension of the algorithm to treat water, to find optimal parameters for the overlap size and finally to include adaptivity of the scheme.

REFERENCES

[1] P. Koumoutsakos, U. Zimmerli, T. Werder, and J. H. Walther, ASME/SPIE handbook of Nanotechnology in press (2003).

[2] T. Werder *et al.*, J. Phys. Chem. B **107**, 1345 (2003).

[3] J. H. Walther, T. Werder, R. L. Jaffe, and P. Koumoutsakos, Phys. Rev. E accepted (2003).

[4] A. L. Garcia, J. B. Bell, W. Y. Crutchfield, and B. J. Alder, J. Comput. Phys. **154**, 134 (1999).

[5] N. G. Hadjiconstantinou, J. Comput. Phys. **154**, 245 (1999).

[6] E. G. Flekkøy, G. Wagner, and J. Feder, Europhys. Lett. **52**, 271 (2000).

[7] R. Delgado-Buscalioni and P. V. Coveney, Phys. Rev. E **67**, 046704 (2003).

[8] N. G. Hadjiconstantinou, A. L. Garcia, M. Z. Bazant, and G. He, J. Comput. Phys. **187**, 274 (2003).

[9] R. Delgado-Buscalioni and P. V. Coveney, J. Chem. Phys. **119**, 978 (2003).

[10] G. Ciccotti and A. Tenenbaum, J. Stat. Phys. **23**, 767 (1980).

[11] E. Matteoli and G. Ali Mansoori, J. Chem. Phys. **103**, 4672 (1995).

[12] R. Tehver, F. Toigo, J. Koplik, and J. R. Banavar, Phys. Rev. E **57**, R17 (1998).

[13] S. V. Patankar and D. B. Spalding, Int. J. Heat Mass Transfer **15**, 1787 (1972).

[14] STAR-CD Version 3.1A. Manual, 1999.

[15] J. H. Walther, R. Jaffe, T. Halicioglu, and P. Koumoutsakos, J. Phys. Chem. B **105**, 9980 (2001).